Effect of oxygen content on magnetic properties of layered cobaltites $PrBaCo_2O_{5+\delta}$

Shraddha Ganorkar,[1] K. R. Priolkar,[1,a)] P. R. Sarode,[1] and A. Banerjee[2]
[1]*Department of Physics, Goa University, Taleigao Plateau, Goa 403 206, India*
[2]*UGC-DAE Consortium for Scientific Research, University Campus, Khandwa Road, Indore 452 001, India*

(Received 18 June 2011; accepted 4 August 2011; published online 15 September 2011)

The effect of oxygen content on the magnetic properties of the layered perovskites has been investigated. The samples, $PrBaCo_2O_{5+\delta}$ ($0.35 \leq \delta \leq 0.80$), were prepared by sol-gel method and characterized by X-ray diffraction and dc magnetization. A detailed magnetic phase diagram for $PrBaCo_2O_{5+\delta}$ is presented. It is found that unlike in the case of heavier rare-earths, ferromagnetic interactions are present at all temperatures below T_C and even in the antiferromagnetically ordered phase. Moreover, in compounds with lower oxygen content, short range ferromagnetic interactions are present even above T_C. This dependence of magnetic properties on oxygen content in these layered perovskites has been linked to the changes in polyhedra around the Co ions. © *2011 American Institute of Physics*. [doi:10.1063/1.3633521]

I. INTRODUCTION

$RBaCo_2O_{5+\delta}$, (R = rare earth elements; $0 \leq \delta \leq 1$) type double perovskites have attracted considerable attention due to considerably high magnetoresistance associated with insulator to metal transition. A strong overlap of the unfilled, and therefore magnetic, *3d* electron orbitals with oxygen *2p* orbitals in these compounds makes them display strong correlation between crystallographic, magnetic, and transport properties. The oxygen content can also be tailored from $\delta = 0$ to $\delta = 1$ by appropriate heat treatment in different atmospheres.[1] The widely accessible oxygen nonstoichiometry and a strong tendency of oxygen vacancies to order in 112-type cobaltites make structural, transport, and magnetic properties depend not only upon oxygen content itself, but also on the synthesis history.[2]

The role of oxygen content is crucial in this family. Both, the mean valence of Co ions and the oxygen coordination around Co are controlled by it. The strength of the crystal field that determines the spin state of Co ions depends on the type of coordination cage surrounding Co ions. Furthermore, according to Goodenough-Kanamori rules, the superexchange magnetic interactions are determined by the orbital occupancy of the outermost *d*-electrons. Consequently, the magnetic and transport properties of these compounds are strongly influenced by the oxygen content and the environment of Co ions. Another factor that is reported to play a role in magnetic properties of these double perovskites is the ordering of oxygen vacancies. The vacancy ordering is dependent on synthesis history.[2] It is reported that oxygen disorder favors ferromagnetic or a canted antiferromagnetic ground state.[2,13,26]

The $RBaCo_2O_{5.5}$, in particular, displays a variety of interesting phenomena including metal insulator transition,[1,3] spin state transition,[4,5] charge ordering,[6,7] and giant magnetoresistance.[7,8] The crystal structure consists of layers of CoO_2 - BaO - $RO_{0.5}$ - CoO_2 stacked along the *c*-axis of an orthorhombic lattice. Due to an alternation of CoO_5 square pyramids and CoO_6 octahedra along the *b* axis leads to its doubling. The CoO_6 octahedra and CoO_5 pyramids in these double perovskites are found to be heavily distorted,[9,10] which leads to the presence of a variety of Co^{3+} spin states[11,12] as a function of crystallographic environment and temperature.

Furthermore, the magnetic properties are quite complex and the compounds display both ferromagnetic and antiferromagnetic transitions.[13–15] Just below T_{MI} the compounds undergo a paramagnetic (PM) to ferro (ferri)magnetic (FM) transition followed by a FM to antiferromagnetic (AFM1) transition that is accompanied by an onset of strong anisotropic magneto-resistive effects. This is also an AFM1 to second antiferromagnetic (AMF2) phase transition. The mechanism of such magnetic transformations at low temperatures is still not properly understood. It is also not clear why subtle changes in oxygen content should cause drastic changes in magnetic properties.[16,17] On the basis of neutron diffraction[13,18–20] and macroscopic measurements,[21] various contradicting magnetic structures, different spin states of Co^{3+} ions as well as spin state ordering (SSO) have been proposed. Muon-spin relaxation (μSR) studies reveal that irrespective of the rare earth ion, a homogeneous FM phase with ferrimagnetic SSO of intermediate spin (IS) and high spin (HS) states develops through two first order phase transitions into phase separated AFM1 and AFM2 phases with different types of antiferromagnetic SSO.[15] Density functional calculations[11,22] and resonant photoemission studies[23] suggest that there is a strong hybridization between O-2*p* and Co-3*d* orbitals with a narrow charge transfer gap near Fermi level. With increasing temperature, the pd_σ hybridized hole in the O-2*p* valence band suffers a gradual delocalization leading to successive magnetic transitions and spin reorientations.

In this work we focus our attention on the role of oxygen content on magnetic properties of these double perovskites.

a)Electronic mail: krp@unigoa.ac.in.

Oxygen content not only affects the valence of Co ions but also the local coordination around it. Such studies are limited to cobalt double perovskites with smaller rare-earth ions like Sm, Eu, and Gd.[24,25] Here the ground state is an antiferromagnetic insulating phase for $\delta \sim 0.5$. Nanoscopic phase separation exists for lower values of δ while ferrimagnetic order is prevalent for higher values of δ. A larger rare-earth ion like Pr, will affect the strength of the crystal field experienced by Co ions and therefore influence the magnetic properties. An understanding of magnetic properties is important from the point of view of both basic physics and probable applications. Therefore, we report here a detailed study of magnetic properties of $PrBaCo_2O_{5+\delta}$, $(0.35 \leq \delta \leq 0.80)$ prepared under very similar synthesis conditions.

II. EXPERIMENTAL

The polycrystalline samples of $PrBaCo_2O_{5+\delta}$ were prepared by sol-gel method. Stoichiometric amounts of Pr_6O_{11}, $BaCO_3$, and $Co_2(NO_2).6\ H_2O$ were dissolved in nitric acid. Citric acid was added to the above solution as a complexing agent. The solution was then heated at 353 K to form a gel that was subsequently dried at 433 K to remove the solvent. This precursor was ground, pelletized, and heated at 1073 K for 4 h followed by annealing at 1323 K for 24 h and slow cooling at the rate of 1°/min to room temperature to get the required sample. This as-synthesized sample had an oxygen stoichiometry of $\delta = 0.80$ as determined by iodometric titration analysis. For iodometric titration, 15 mg of sample and solid KI were dissolved in 1 N HCl, and quickly titrated against 0.01 N sodium thiosulphate using starch as an indicator. Inert atmosphere was maintained by adding sodium carbonate during titration. The oxygen content was calculated from the amount of sodium thiosulphate consumed to get end point. At least three to five titrations were performed on each sample, and the maximum probable error in the oxygen content was found to be less than ± 0.01. Oxygen content of each compound in the series was varied by individually annealing the samples in argon atmosphere at different temperatures. In particular, the samples with $\delta = 0.67$, 0.58, 0.5, and 0.43 were annealed, respectively, at 673 K, 873 K, 1073 K, and 1173 K for 36 h while the sample with $\delta = 0.35$ was annealed twice at 1073 K for 36 h. Iodometric titration was again used to determine the oxygen content of these samples. The samples were deemed to be phase pure, as X-ray diffraction (XRD) data recorded using Rigaku D-Max IIC X-ray diffractometer in the range of $20° \leq 2\theta \leq 80°$ using Cu K_α radiation showed no impurity reflections. The diffraction patterns were Rietveld refined using FULLPROF suite, and structural parameters were obtained. Magnetization measurements were carried out as a function of temperature and magnetic field using a Quantum Design superconducting quantum interference device (SQUID) magnetometer and VSM at different applied field values of 100, 1000, and 10 000 Oe, in the temperature range of 10 K to 300 K. The sample was initially cooled from room temperature to the lowest temperature (10 K) in zero applied field. Magnetization was recorded while warming under an applied field (zero-field cooled (ZFC)) and subsequent cooling field-cooled cooling (FCC) and warming (FCW) cycles. The isothermal magnetization M(H) curves were recorded at various temperatures in the field range of $\pm$ 7 T and $\pm$ 14 T.

III. RESULTS

The structure of Co based double perovskites is known to depend on the oxygen content $5 + \delta$. In general, there are three structural regimes reported.[2] The hole doped region $(0.7 \leq \delta \leq 1)$ wherein the structure is tetragonal, the intermediate region $(0.3 \leq \delta \leq 0.7)$, which is characterized by doubling of b axis due to ordering of the Co ions and orthorhombic structure, and the electron doped region $(0 \leq \delta \leq 0.3)$ with the compounds having tetragonal structure. The limits of structural transition are not strict and often depend on the rare-earth ion. With the change in oxygen content, the coordination geometry around Co ions also changes from octahedral ($\delta \approx 1$) to square pyramidal ($\delta \approx 0$). Fig. 1 displays XRD pattern of as-prepared $PrBaCo_2O_{5.80}$ sample and Ar annealed sample $PrBaCo_2O_{5.35}$. Rietveld refinement of XRD pattern of $PrBaCo_2O_{5.80}$ confirms the formation of a largely single phase sample with 112 type tetragonal unit cell belonging to *P4/mmm* space group. A very minor impurity phase is detected with peaks around $2\theta \sim 29°$ and 31° that can be ascribed to unreacted Pr-oxides (Pr_2O_3, Pr_6O_{11}). These impurity peaks are seen only in the two end members and are not present in any of the intermediate compositions. The tetragonal structure preserves up to $\delta = 0.67$. Samples with oxygen content ≤ 5.58 crystallize in orthorhombic structure with *Pmmm* space group and 122 type unit cell. This change in structural symmetry is reflected by the splitting of (200) peak at $2\theta \approx 46°$ as can be seen in Fig. 2. Due to tetragonal to orthorhombic transition and subsequent doubling of unit cell along the b-axis, the (200) reflection splits into two distinct (200) and (040) Bragg peaks. A plot of variation of lattice parameters with oxygen content is presented in Fig. 3 From this plot, it is observed that, with the decrease in oxygen content, the lattice parameters a and b deviate away from each other upon the tetragonal to orthorhombic phase transition indicating an increase in orthorhombic

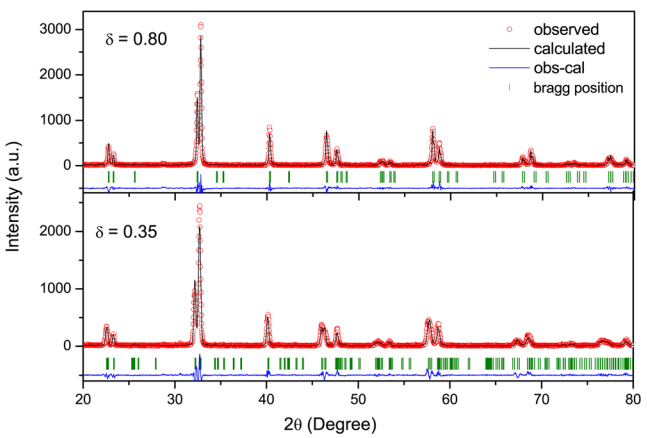

FIG. 1. (Color online) Rietveld refinement XRD patterns of $PrBaCo_2O_{5+\delta}$, $\delta = 0.80$ and 0.35. Circles represent experimental data, continuous line through the data is the fitted curve, and the difference pattern is shown at the bottom as a solid line.

distortion, $O_s = (a-b)/(a+b)$. This distortion is found to be maximum for $\delta = 0.43$ (Fig. 3(b)). On the other hand, c parameter remains nearly constant in the regions $0.8 \leq \delta \leq 0.6$ and $\delta < 0.4$ and exhibits a decrease for intermediate values of δ. Such a trifurcation of lattice parameters is also seen in the case of $GdBaCo_2O_{5+\delta}$.[24] It must be mentioned here that the regions indicated above are based on gross structural symmetry, and local structural effect could play an important role in deciding the magnetic properties.

The temperature dependence of magnetization M(T) measured at 100 Oe is shown in Fig. 4. The ZFC and FC magnetization curves of all samples except $\delta = 0.80$ show PM to FM transition followed by a decrease in magnetization, which, based on neutron diffraction results,[13] is ascribed to a FM to AFM transition. The compound with $\delta = 0.80$ exhibits a PM to FM transition at $T_C = 148$ K. There is, however, a large difference between ZFC and FC magnetization curves of this compound. Studies on oxygen rich $PrBaCo_2O_{5+\delta}$ indicate that compounds with $\delta = 0.9$ and 0.85 order ferromagnetically while that with $\delta = 0.75$ orders antiferromagnetically at 175 K, which can be transformed to FM state under magnetic field.[27] Hence, the difference between ZFC and FC magnetization curves for $\delta = 0.8$ sample can be ascribed to the presence of competing magnetic interactions.

A closer examination of M(T) curves indicates presence of a few more magnetic transitions at low temperatures. For $\delta = 0.80$ apart from the PM to FM transition, another transition is visible at $T_{R1} \sim 50$ K that has not been hitherto reported. This transition is also present in other compounds (see insets (i) in Figs. 4(a)–4(d) and insets (ii) in Figs. 4(e)

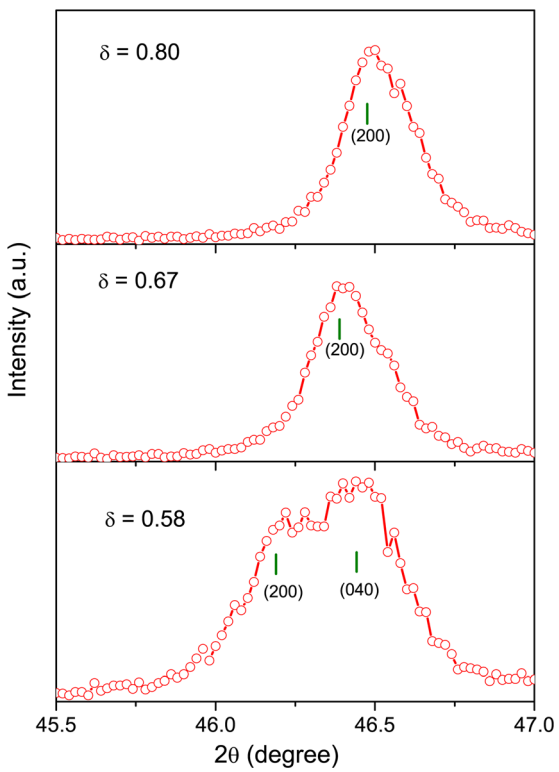

FIG. 2. (Color online) The (200) Bragg reflection and its splitting to (200) (040) upon tetragonal to orthorhombic transition in $PrBaCo_2O_{5+\delta}$.

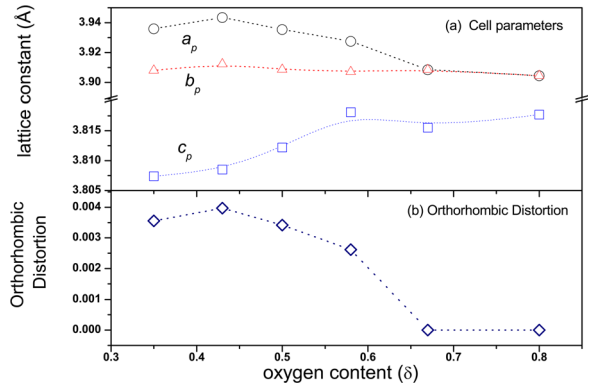

FIG. 3. (Color online) Variation of cell parameters (a) and orthorhombic distortion (b) in $PrBaCo_2O_{5+\delta}$ as a function of oxygen content (δ).

and 4(f)). The transition temperature T_{R1} shows a tendency to increase with decreasing δ followed by a sharp rise to about 140 K for $\delta = 0.43$. It may be noted that this particular compound has maximum orthorhombic distortion. The transition temperature decreases again to about 50 K for $\delta = 0.35$. Muon spin relaxation (μSR) studies on $NdBaCo_2O_{5.5}$ attribute the transition around 50 K to a magnetic phase transition.[28]

Furthermore, the magnetization behavior of compounds with $\delta = 0.43$ and 0.35 is even more complex. For example, in case of $\delta = 0.43$, a double hump structure is observed just below the PM to FM transition. Additionally an upturn in magnetization is observed at $T_{R2} \sim 17$ K. This can be clearly seen in the inset (ii) of Figs. 4(e) and 4(f) and could be ascribed to paramagnetic contribution of the rare-earth ion that is amplified in these two compositions due to the presence of Pr-oxide impurity phase seen in XRD. Furthermore, another new transition around 300 K $= T_{R3}$ (see inset (i) of Figs. 4(e) and 4(f)) is observed for $\delta = 0.43$ and 0.35.

Second aspect that stands out is the low values of magnetization in compounds with $\delta < 0.8$. Different hypotheses have been considered to explain the low value of the magnetic moment. Firstly, it could be due to the presence of low spin ($S = 0$) Co^{3+} ions as majority species. However, optical studies on Eu based double perovskites discounts this possibility.[29] The resulting small total magnetization observed at low temperature could be due to ferrimagnetic ordering or mutually orientated moments of $Co^{2+/3+}$ ions in the nonequivalent pyramidal and octahedral sites. A third hypothesis is based on the coexistence of ferromagnetic and an antiferromagnetic phase or on segregation of a FM phase in the antiferromagnetic matrix in the form of ferromagnetic domains. This phase separation scenario is also observed for $GdBaCo_2O_{5+\delta}$.[24] In this case, the application of the magnetic field continuously transforms the antiferromagnetic state into ferromagnetic state.

To investigate the effect of magnetic field on the above magnetic transition temperatures and magnetization in general, M(T) has been recorded at 1000 Oe and 1 T during FCC and FCW cycles for the samples with $\delta = 0.80$, 0.58, 0.50, and 0.35. A small amount of thermal hysteresis that increases with decreasing δ is still observed below T_C even in fields of 1 T confirming the presence of a complex

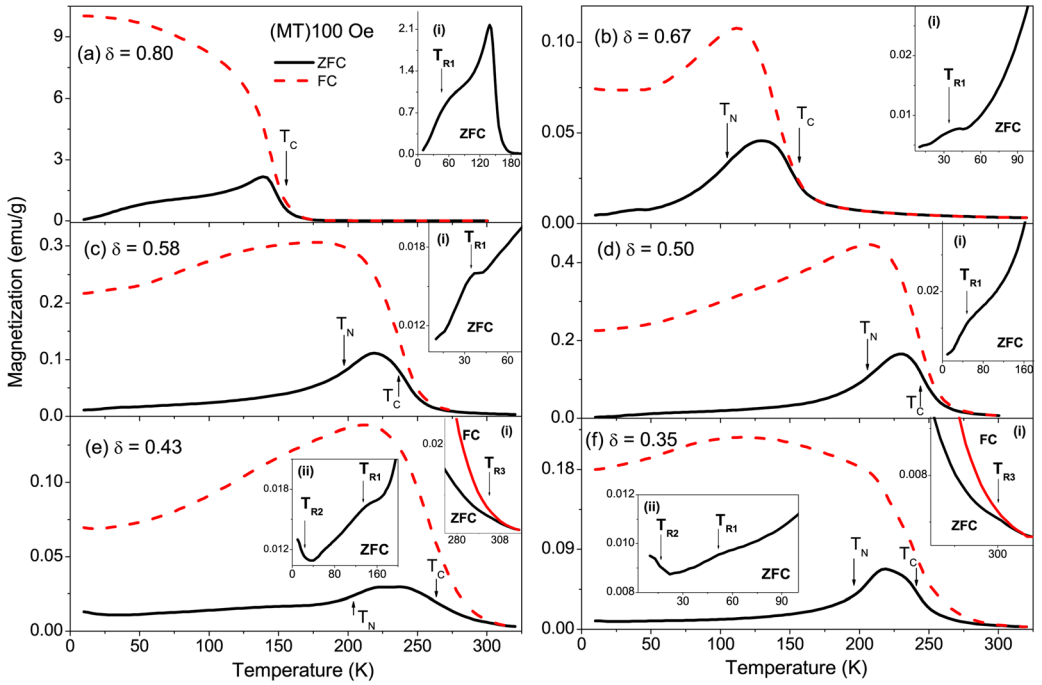

FIG. 4. (Color online) Magnetization as a function of temperature for $PrBaCo_2O_{5+\delta}$ compounds recorded in an applied field of 100 Oe. The solid lines denote magnetization recorded during the ZFC cycle while the dashed curve represents magnetization during the FC cycle. Insets show the details transition regions.

magnetic ground state as was evident from magnetization curves at 100 Oe. Furthermore, the absence of saturation is another evidence for the presence of competing FM and AFM interactions in these compounds. A closer look at Fig. 5 indicates a presence of a crossover between FCC and FCW curves (see insets (i) and (ii) of Figs. 5(a)–5(d)). At low temperatures the FCC curves lie below the FCW curves. As the temperature is increased, the FCC curves crossover and lie above the FCW curves. This crossover temperature is seen to be dependent on oxygen content. It is observed that this crossing temperature is maximum for $\delta = 0.50$ (202 K), and lower for $\delta = 0.58$ (176.4 K), 0.35 (174 K), while no such feature is observed for $\delta = 0.80$. In the case of $\delta = 0.35$, a similar crossover is also seen below 298 K indicating a presence of a short range magnetic transition.

The isothermal magnetization M(H) recorded at 10 K and in the vicinity of T_C and T_N for compounds having $\delta = 0.80$, 0.58, and 0.50 compounds and at 250 K and 300 K for $\delta = 0.35$. The M(H) for $\delta = 0.80$ is presented in Fig. 6. A clear hysteresis loop signifying the presence of ferromagnetism is observed at 10 K. The magnetization, however, does not saturate even up to 14 T indicating a presence of strong magnetic anisotropy or a competing AFM state. The hysteretic behavior persists up to 150 K though the coercive field decreases with increasing temperature before vanishing at $T_C = 150$ K (top left inset of Fig. 6(c)). M(H) curve at 300 K shown in the bottom left inset of Fig. 6(c) indicates the sample to be paramagnetic at this temperature. Another notable feature in the hysteresis curves is that the virgin curve lies outside the loop at 100 K and 150 K. This can be attributed to the presence of two different Co ions in the matrix. Due to the presence of Co^{3+} and Co^{4+} ions, there is an electronic phase separation. The ferromagnetism can be attributed to majority Co^{3+} - O - Co^{4+} superexchange interactions in agreement with Goodenough-Kanamori rule.[30] While AFM can be due to minority Co^{3+} - O - Co^{3+} superexchange interaction. In the presence of magnetic field, the contribution from FM interactions grows at the expense of AFM interaction leading to the initial magnetization curve to lie outside the main loop.

The M(H) curves for $PrBaCo_2O_{5.5}$ and $PrBaCo_2O_{5.58}$ are presented in Fig. 7. The behaviors of the two samples being very similar are discussed together. The main point is that although the samples are reported to undergo AFM transition, ferromagnetic hysteresis loop is observed at all temperatures below T_C. Further, for the sample with $\delta = 0.5$, isothermal magnetization measured at 300 K (Inset in Fig. 7(a)) shows a slight curvature indicating presence of short range ferromagnetic interactions well above T_C. In the case of both samples, coercive field increases with decrease in temperature indicating strengthening of FM interactions. However, no saturation of magnetization is observed even at lowest temperature and maximum field of measurement in the case of these compounds. The continuous increase in magnetization with field could also be attributed to paramagnetic contribution of Pr ions. However, this contribution would have been reversible, in contrast to the obtained result. The hysteresis loop at 10 K shows a clear irreversibility right up to fields = 14 T. This indicates the presence of competing ferro- and antiferromagnetic interactions in the two samples. Moreover, it is clear that the magnetization is induced by the applied field rather than being of spontaneous nature.

In the case of a compound with low oxygen content, ($\delta = 0.35$), M(H) curves at 300 K and 250 K are presented in Fig. 8. It may be noted that both temperatures are above its T_C. The magnetization curve at 300 K exhibits a curvature toward the horizontal axis. Such a behavior can be attributed to the presence of short range ferromagnetic interactions.

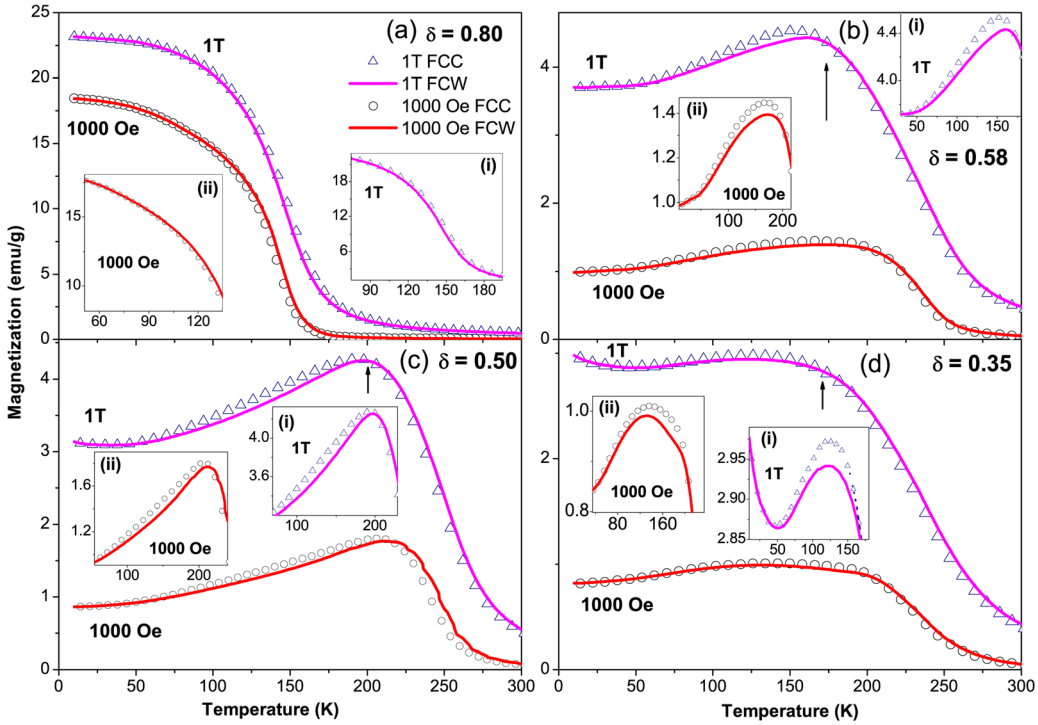

FIG. 5. (Color online) Temperature dependence of magnetization recorded at 1000 Oe and 1 T for FCC and FCW cycles. The crossing FCC and FCW curves is presented more clearly in the insets.

Furthermore, the M(H) curve at 250 K exhibits a narrow hysteresis loop ($m_0 \simeq 0.21$ emu/g, $H_C \simeq 856$ Oe). This observation clearly indicates the transition T_{R3} to be ferromagnetic in nature. This weak FM ordering could arise due to Co^{2+} - O - Co^{3+} interactions.

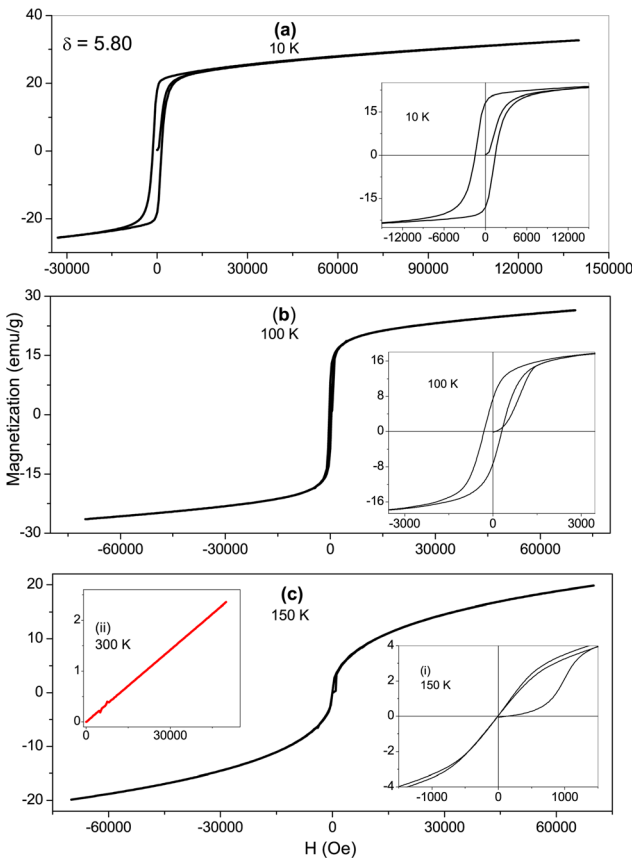

FIG. 6. (Color online) Hysteresis loops for $PrBaCo_2O_{5.80}$ recorded at (a) 10 K, (b) 100 K, and (c) 150 K. The same data on a magnified scale are shown in the insets. M vs H data at 300 K is presented in inset (ii).

IV. DISCUSSION

It is quite evident from the above studies that δ has a great influence on magnetic transition temperatures. The variation of these transition temperatures as identified from the magnetization curves recorded at 100 Oe as a function of oxygen content (δ) is depicted in Fig. 9. It is quite evident that both T_C and T_N increase as δ decreases from 0.67 to 0.35. Though the magnetization of sample with $\delta = 0.8$ does not show a presence of an antiferromagnetic transition, the wide separation between ZFC and FC magnetization curves and

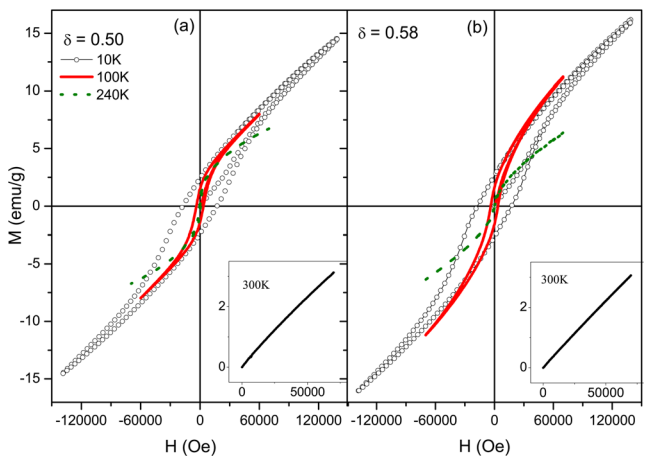

FIG. 7. (Color online) Isothermal magnetization curves of $PrBaCo_2O_{5+\delta}$.(a) $\delta = 0.50$ and (b) $\delta = 0.58$ recorded at 10 K, 100 K, and 240 K. The initial magnetization curve at 300 K is shown in insets (a) and (b).

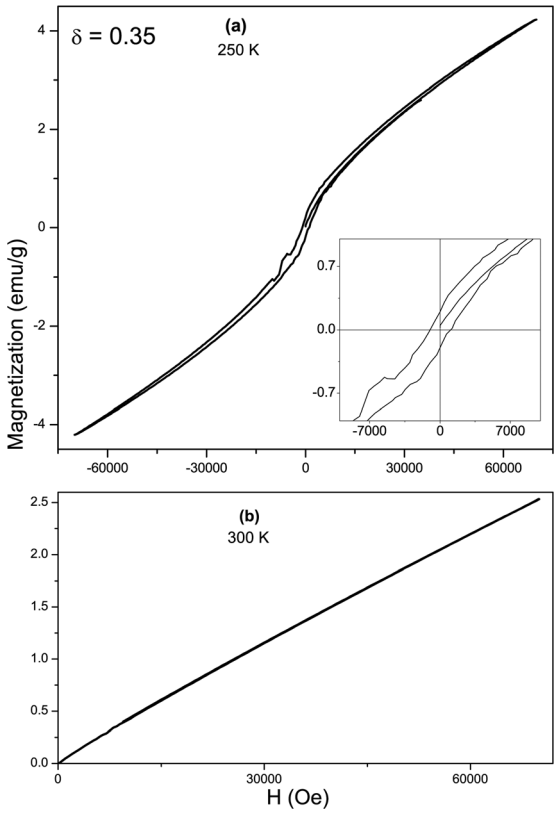

FIG. 8. Magnetization as a function of magnetic field for $PrBaCo_2O_{5.35}$ recorded at (a) 250 K with the inset showing an expanded view of the hysteresis loop and (b) the data recorded at 300 K.

the nature of magnetic hysteresis loops clearly show the presence of competing AFM and FM interactions. It is also seen that all the compounds undergo another magnetic transition T_{R1} at lower temperatures. This transition appears to be related to orthorhombic distortion. In addition, the compounds with $\delta \leq 0.43$ exhibit two new magnetic transitions, T_{R2} and T_{R3}. The presence of hysteresis in M(H) loops of $\delta = 0.35$ well above its T_C tends to indicate that the transition at T_{R3} is ferromagnetic. Based on these, the nature of magnetic order present in different temperature zones as a function of oxygen content is indicated in Fig. 9. The magnetic

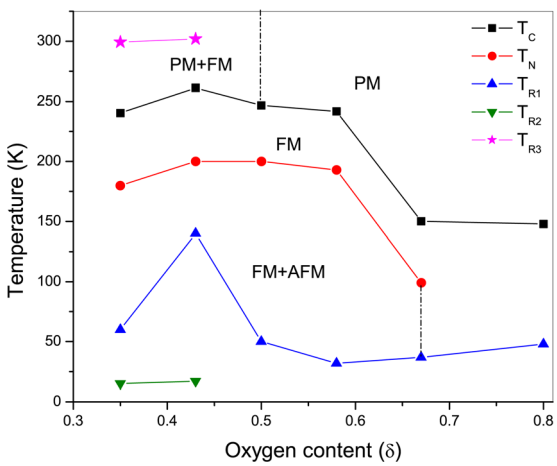

FIG. 9. (Color online) Effect of oxygen content on various transition temperatures estimated from 100 Oe ZFC magnetization data for $PrBaCo_2O_{5+\delta}$.

phase diagram so constructed is quite different from that obtained for cobalt double perovskites containing heavier rare-earth ions like Eu and Sm.[25] Although the Pr containing double perovskites undergoes more than one magnetic transition that include PM to FM and FM to AFM transitions, the pure antiferromagnetic phase found in perovskites with heavier rare-earths is absent in $PrBaCo_2O_{5+\delta}$. Here, ferromagnetism prevails and co-exists with antiferromagnetic phase right down to the lowest temperature studied. It appears that for compounds with lower values of δ, ferromagnetic phase is present as a minor phase or domains embedded in an antiferromagnetic matrix, while in the case of $\delta = 0.8$, the compound is ferromagnetic due to Co^{3+} - O - Co^{4+} superexchange interactions with a minor antiferromagnetic phase arising due to Co^{3+} - O - Co^{3+} interactions.

A plot of various Co-O bond distances obtained from Rietveld refinement of room temperature XRD patterns against oxygen content δ is presented in Fig. 10. It can be seen that the Co-O planar bond distances belonging to both the polyhedra increase when the structure changes from tetragonal to orthorhombic. Further, the variation of the apical bond distances indicate that as δ decreases, the octahedra shrink from top and get elongated from bottom. An increase in planar Co-O bond length with structural transition indicates the tilting of polyhedra. Tilting of polyhedra with a decrease in oxygen content results in increased distortion of the CoO polyhedra. Distortion of polyhedra reflects an increased orthorhombic distortion with decreasing δ. Increased distortions will also result in a decrease in Co - O - Co inter polyhedral bond angle and thereby favor antiferromagnetic ordering due

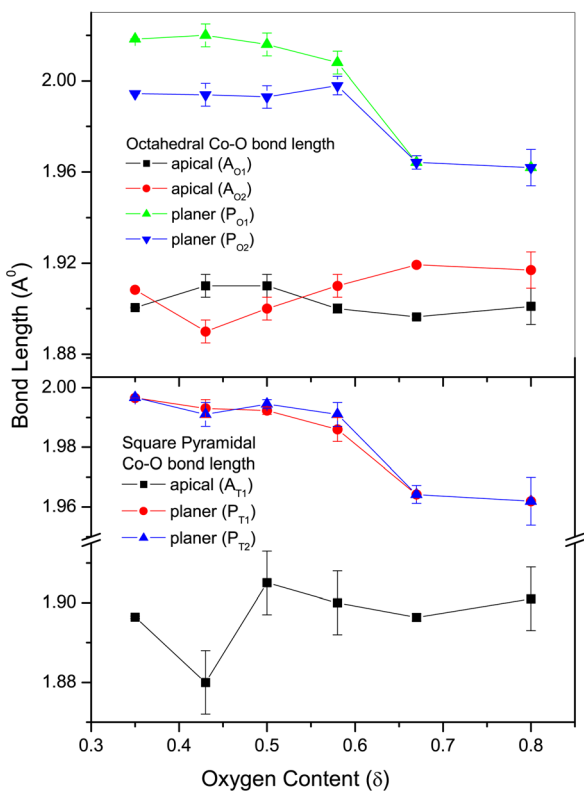

FIG. 10. (Color online) Variation of Co-O bond lengths obtained from room temperature XRD data for octahedral and square pyramidal coordination of $PrBaCo_2O_{5+\delta}$ as a function of oxygen content δ.

to localization of charge carriers. However, the presence of a relatively larger rare-earth ion like Pr tends to minimize these Co-O polyhedral distortions. Thus, resulting in the ferromagnetic phase persisting right down to the lowest temperature. A detailed investigation of local structural distortions and their variation as a function of temperature will help in understanding the magnetic phase diagram.

V. CONCLUSION

In summary, there exists a transition from tetragonal to orthorhombic structure with a decrease in oxygen content. All the samples have a complex magnetic ground state due to competing ferromagnetic and antiferromagnetic interactions. Unlike in the case of heavier rare-earths where a pure antiferromagnetic ordering has been observed, the phase below T_N in $PrBaCo_2O_{5+\delta}$ is a mixture of antiferromagnetic and ferromagnetic order. In addition to T_C and T_N, all the compounds undergo another magnetic transition at T_{R1}. The temperature of this transition is highest for the compound with the largest orthorhombic distortion indicating it to be linked to structural degrees of freedom. Compounds with lower oxygen content ($\delta \leq 0.43$), undergo two more magnetic transitions—one around 15 K (T_{R2}) and the other at around 300 K (T_{R3}). The presence of magnetic hysteresis indicates the transition at T_{R3} to be ferromagnetic in nature. The multiple magnetic transitions can be ascribed to the distortions of CoO polyhedra arising due to oxide ion deficiency.

ACKNOWLEDGMENTS

Authors would like to acknowledge financial assistance from the Council for Scientific and Industrial Research, New Delhi under the project EMR-II/1099. S.G. acknowledges the travel assistance and local hospitality extended to her by Centre Director, UGC-DAE Consortium, Indore.

[1]A. Maignan, C. Martin, D. Pelloquin, N. Nguyen, and B. Raveau, J. Solid State Chem. **142**, 247 (1999).
[2]S. Streule, A. Podlesnyak, J. Mesot, M. Medared, K. Conder, E. Pomjakushina, E. Mitberg, and V. Kozhevnikov, J. Phys: Condens. Matter **17**, 3317 (2005).
[3]C. Martin, A. Maignan, D. Pelloquin, N. Nguyen, and B. Raveau, Appl. Phys. Lett. **71**, 1421 (1997).
[4]Y. Moritomo, T. Akimoto, M. Takeo, A. Machida, E. Nishibori, M. Takata, M. Sakata, K. Ohoyama, and A. Nakamura, Phys. Rev. B **61**, R13325 (2000).
[5]M. Respaud, C. Frontera, J. García-Muñoz, A. G. M. Aranda, B. Raquet, J. Broto, H. Rakoto, M. Goiran, A. Llobet, and J. Carvajal, Phys. Rev. B **64**, 214401 (2001).
[6]T. Vogt, P. M. Woodward, P. Karen, B. A. Hunter, P. Henning, and A. R. Moodenbaugh, Phys. Rev. Lett. **84**, 2969 (2000).
[7]E. Suard, F. Fauth, V. Caignaert, I. Mirebeau, and G. Baldinozziet, Phys. Rev. B **61**, R11871 (2000).
[8]I. Troyanchuk, N. Kasper, and D. D. Khalyavin, Phys. Rev. Lett. **80**, 3380 (1998).
[9]D. D. Khalyavin, S. Barilo, S. Shiryaev, G. Bychkov, I. Troyanchuk, A. Furrer, P. Allenspach, S. Szymczak, and R. Szymczak, Phys. Rev. B **67**, 214421 (2003).
[10]E. Pomjakushina, K. Conder, and V. Pomjakushin, Phys. Rev. B **73**, 113105 (2006).
[11]H. Wu, Phys. Rev. B **64**, 92413 (2001).
[12]E. Zhitlukhina, K. Lamonova, S. Orel, P. Lemmens, and Y. Pashkevich, J. Phys. Condens. Matter **19**, 156216 (2007).
[13]C. Frontera, J. L. García-Muñoz, A. Carrillo, M. A. G. Aranda, I. Margiolaki, and A. Caneiro, Phys. Rev. B **74**, 054406 (2006).
[14]C. Frontera, J. L. García-Muñoz, and A. Carrillo, Phys. Rev. B **70**, 184428 (2004).
[15]H. Luetkens, M. Stingaciu, Y. Pashkevich, K. Conder, E. Pomjakushina, A. Gusev, K. Lamonova, P. Lemmens, and H. Klauss, Phys. Rev. Lett. **101**, 017601 (2008).
[16]W. Kim, E. Chi, H. Choi, N. Hur, S. Oh, and C. Ri, Solid State Commun. **116**, 609 (2000).
[17]J. Burley, J. F. Mitchell, S. Short, D. Millar, and Y. Tang, J. Solid State Chem. **170**, 339 (2003).
[18]V. Plakhty, P. Chernenkov, S. Barilo, E. Podlesnyak, E. Pomjakushina, E. Moskvin, and S. Gavrilov, Phys. Rev. B **71**, 214407 (2005).
[19]F. Fauth, E. Suard, V. Caignaert, and I. Mirebeau, Phys. Rev. B **66**, 184421 (2002).
[20]M. Soda, Y. Yasuij, M. Ito, S. Iikubo, and M. Sato, J. Phys. Soc. Jpn. **72**, 1729 (2003).
[21]A. Taskin, A. N. Lavrov, and Y. Ando, Phys. Rev. Lett. **90**, 227201 (2003).
[22]H. Wu, J. Phys.: Condens. Matter **15**, 503 (2003).
[23]W. Flavell, A. Thomas, D. Tsoutsou, A. Mallick, M. North, E. Seddon, C. Cacho, A. Malins, S. Patel, R. Stockbauer, R. Kurtz, P. Sprunger, S. Barilo, S. Shiryaev, and G. Bychkov, Phys. Rev. B **70**, 224427 (2004).
[24]A. Taskin, A. Lavrov, and Y. Ando, Phys. Rev. B **71**, 134414 (2005).
[25]M. Motin Seikh, A. K. Kundu, V. Caignaert, V. Pralong, and B. Raveau, J. Appl. Phys. **109**, 093916 (2011);M. M. Seikh, C. Simon, V. Caignaert, V. Pralong, M. B. Lepetit, S. Boudin, and B. Raveau, Chem. Mater. **20**, 231 (2008).
[26]C. Frontera, J. L. García-Muñoz, C. Ritter, and A. Canerio, J. Phys.: Condens. Matter **20**, 104228 (2008).
[27]J. L. García-Muñoz, C. Frontera, A. Llobet, A. Carrillo, C. Caneiro, M. A. G. Aranda, M. Respaud, C. Ritter, and E. Dooryee, J. Magn. Magn. Mater. **272–276**, 1762 (2004).
[28]A. Jarry, H. Luetkens, Y. Pashkevich, M. Stingaciu, E. Pomjakushina, K. Conder, P. Lemmens, and H. Klaus, Physica B **404**, 765 (2009).
[29]A. A. Makhnev, L. V. Nomerovannaya, A. O. Tashlykov, S. N. Barilo, and S. V. Shiryaev, Phys. Solid State **49**, 894 (2007).
[30]J. Goodenough, *Magnetism and the Chemical Bond* (Wiley-Interscience, New York, 1963).